0026-895X/01/6003-450–461$3.00
MOLECULAR PHARMACOLOGY
Vol. 60, No. 3
862/925123
Mol Pharmacol 60:450–461, 2001
Printed in U.S.A.

Apoptosis Induced by the Homocamptothecin Anticancer Drug BN80915 in HL-60 Cells

AMELIE LANSIAUX, MICHAEL FACOMPRÉ, NICOLE WATTEZ, MARIE-PAULE HILDEBRAND, CHRISTINE BAL, DANIÉLE DEMARQUAY, OLIVIER LAVERGNE, DENNIS C. H. BIGG, and CHRISTIAN BAILLY

Institut National de la Santé et de la Recherche Médicale U-524 and Laboratoire de Pharmacologie Antitumorale du Centre Oscar Lambret, Institut de Recherche sur le Cancer de Lille, Lille, France (A.L., M.F., N.W., M.-P.H., C.B., C.B.); and Institut Henri Beaufour, Les Ulis, France (D.D., O.L., D.C.H.B.)

Received February 5, 2001; accepted May 23, 2001

This paper is available online at http://molpharm.aspetjournals.org

ABSTRACT

The homocamptothecin (hCPT) derivative BN80915 containing a seven-membered lactone ring represents one of the most potent topoisomerase I inhibitors described. This anticancer agent, currently undergoing phase I clinical trials, has been shown to produce a greater number of DNA strand breaks than conventional camptothecins with a six-membered lactone ring. To shed light on the mechanism of action of hCPT at the cellular level, we compared the effects of BN80915 and the classic camptothecin SN-38, the active metabolite of irinotecan, on HL-60 human promyelocytic cancer cells. A variety of biochemical events, at both the mitochondrial and the nuclear levels, were characterized to determine how and to what extent the hCPT derivative can induce apoptotic cell death. The use of cytometry, Western blot analysis, confocal microscopy, and different colorimetric assays enabled us to demonstrate that BN80915 is a potent inducer of apoptosis in HL-60 cells. This induction of apoptosis is associated with cell cycle changes, a marked decrease of intracellular pH, activation of caspase-3 and -8, DNA fragmentation, and externalization of phosphatidylserine lipids but no significant changes of the mitochondrial membrane potential or the expression of Bcl-2. The interconnections between these different events are discussed. Collectively, the results indicate that the superior activity expressed at the topoisomerase I level leads to a more pronounced induction of apoptosis by BN80915 compared with SN-38. The study identifies and delineates signaling factors involved in BN80915-induced apoptosis in HL-60 cells.

Featuring a seven-membered β-hydroxy lactone instead of the six-membered α-hydroxy lactone found in camptothecin (CPT), homocamptothecin (hCPT, Fig. 1) is a promising prototype for the next generation of topoisomerase I targeting agents (Lavergne et al., 1997, 1998). The modified lactone of hCPT hydrolyses slowly and irreversibly, and it circumvents the complications associated with the intrinsic instability of conventional CPTs. Because of the high reactivity of their six-membered lactone, conventional CPTs hydrolyze rapidly and reversibly to reach an equilibrium with their open carboxylate forms, which are essentially inactive. The biologically active lactone form predominates only under acidic conditions, and in plasma the equilibrium is shifted toward the carboxylate form in a species-dependent manner, which is less favorable in humans than in rodents. Upgrading the highly reactive six-membered lactone to a more stable seven-membered ring is achieved without compromising any antitumor activity: hCPT not only remains a potent poison for topoisomerase I (Lesueur-Ginot et al., 1999), it also has a reinforced capacity to stimulate DNA cleavage by topoisomerase I and a broader range of sequence-specific DNA cleavage sites. Whereas both CPT and hCPT stimulate the cleavage by topoisomerase I at T$^{\downarrow}$G sites (the arrow indicates the position of cleavage) hCPT also stabilizes cleavage at sites containing the sequence AAC$^{\downarrow}$G (Bailly et al., 1999). Finally, even under acidic conditions, the hydrolysis of the seven-membered β-hydroxy lactone of hCPT is irreversible, thereby avoiding the risk of hemorrhagic cystitis, a frequent dose-limiting toxicity of some conventional CPTs.

Initial testing of racemic hCPT as well as further evaluation of its enantiomerically pure *R* form has shown hCPT to

This work was performed with the support of research grants (to C.Bailly) from the Institut de Recherches sur le Cancer de Lille and the Ligue Nationale Française Contre le Cancer (Comité du Nord).

ABBREVIATIONS: CPT, camptothecin; hCPT, homocamptothecin; $DiOC_6$, 3-dihexyloxacarbocyanine iodide; JC-1, tetrachloro-tetraethylbenzimidazolcarbocyanine iodide; SNARF-AM, carboxy-seminaphthorhodafluor-1-acetoxymethyl ester; CCCP, carbonyl cyanide *p*-chlorophenylhydrazone; WST1, 4-[3-(4-iodophenyl)-2-(4-nitrophenyl)-2H-5-tetrazolio]-1,3-benzene disulfonate; EthD-1, ethidium homodimer-1; BrdU, 5-bromo-2-deoxyuridine; FITC, fluorescein isothiocyanate; DEVD-pNA, *N*-acetyl-Asp-Glu-Val-Asp-pNA; IETD-pNA, *N*-acetyl-Ile-Glu-Thr-Asp-pNA; PARP, poly(ADP-ribose) polymerase; PBST, phosphate-buffered saline/Tween 20; TUNEL, terminal deoxynucleotidyl transferase–mediated dUTP nick-end labeling; PI, propidium iodide; PS, phosphatidylserine; TPT, topotecan; PAGE, polyacrylamide gel electrophoresis.

be more active than CPT on a panel of tumor cell lines in vitro and in xenograft in vivo models (Lavergne et al., 1997; Lesueur-Ginot et al., 1999). Superior anticancer activities for hCPT versus CPT were also shown using a variety of human colon cancers obtained from surgery and maintained in vitro under histotypical culture conditions (Philippart et al., 2000). The increased antitumor activity is attributed to the higher propensity of hCPT to inhibit topoisomerase I compared with that of CPT. Camptothecin-resistant cells expressing mutated topoisomerase I were found to be highly resistant to hCPT (Bailly et al., 1999; Urasaki et al., 2000). Recently, we found an overall linear relationship between the antiproliferative activities of fluorinated hCPT derivatives and their anti-topoisomerase I properties (Lavergne et al., 2000). One of the most potent hCPT analogs is the bis-fluoro derivative BN80915 (Fig. 1), which has advanced into clinical trials. BN80915 showed remarkable antitumor profiles in vitro (Principe et al., 1999; Philippart et al., 2000; Larsen et al., 2001), and the first results of the phase I clinical trials are encouraging. It is still too early to know whether BN80915 will take its place in the armament against cancer, but it is already clear that the hCPT strategy is highly valuable and will probably lead to the development of a useful antitumor drug. Various hCPT derivatives, including BN80927 (Lavergne et al., 1998), 12-Cl-hCPT (Bailly et al., 2001), and the silylated derivatives homosilatecans (Bom et al., 1998), represent potential hCPT-based candidates for future drug development.

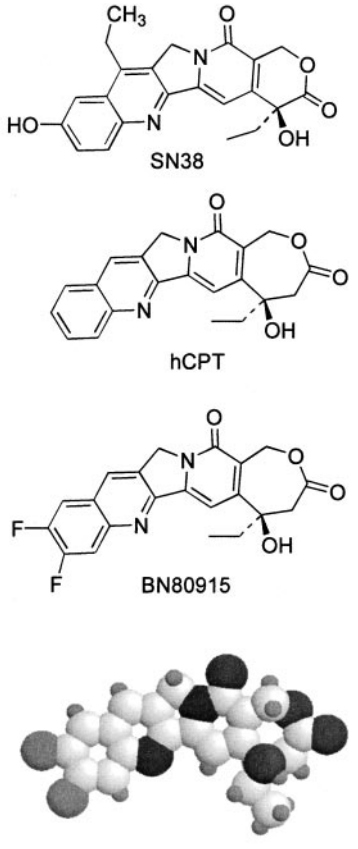

Fig. 1. Structure of SN38, hCPT, and BN80915. An energy-minimized structure of BN80915 is shown. The software programs HyperChem 5.01 (HyperCube, Inc, Gainesville, FL) and Alchemy 2000 (SciVision, Burlington, MA) were used to construct the structure.

Topoisomerase I is the essential molecular target for hCPT (Urasaki et al., 2000). However, if the nuclear target is now well characterized, very little is known, in contrast, concerning the downstream molecular events leading to the cytotoxic action of the drug. To shed light on the mechanism of action of hCPTs at the cellular level, we compared the effects of the tumor-active drug BN80915 and the camptothecin SN-38 on HL-60 human promyelocytic cancer cells. Specifically, we sought to determine how and to what extent the hCPT derivative can induce apoptotic cell death.

Materials and Methods

Drugs and Chemicals

The synthesis of enantiopure BN80915 has been reported recently (Lavergne et al., 2000), and SN-38 was prepared according to a procedure published previously (Sawada et al., 1991). The drugs were dissolved in 5 mM dimethyl sulfoxide and then further diluted with water. The stock solutions of drugs were kept at −20°C and were freshly diluted to the desired concentration immediately before use. Nigericin, 3-dihexyloxacarbocyanine iodide ($DiOC_6$), tetrachloro-tetraethylbenzimidazolcarbocyanine iodide (JC-1), carboxy-SNARF-1-acetoxymethyl ester (SNARF-AM), and carbonyl cyanide *p*-chlorophenylhydrazone (CCCP) were from Molecular Probes, Inc. (Eugene, OR). Oligomycin and 5-bromo-2-deoxyuridine (BrdU) were from Sigma (La Verpillière, France). All other chemicals were analytical-grade reagents.

Cell Cultures and Cell Survival Assay

Human HL-60 promyelocytic leukemia cells were obtained from the American Type Culture Collection (Manassas, VA). Cells were grown at 37°C in a humidified atmosphere containing 5% CO_2 in RPMI 1640 medium supplemented with 10% fetal bovine serum, glutamine (2 mM), penicillin (100 IU/ml), and streptomycin (100 μg/ml). The inhibition of cell proliferation was determined with the use of 4-[3-(4-iodophenyl)-2-(4-nitrophenyl)-2H-5-tetrazolio]-1,3-benzene disulfonate (WST1) colorimetric assay. Cells were seeded in wells containing 2000 cells/80 μl RPMI on a microtiter plate (tissue culture grade, 96 wells, flat bottom) 24 h before treatment. Cells were incubated with 20 μl of the test drug for 4 h over final concentrations ranging from 10^{-8} to 10^{-5} M. The drug-containing medium was then replaced with a drug-free medium, and the incubation was continued for 24 or 72 h. After this incubation period, 10 μl of WST1 labeling reagent was added to each well. Cells were incubated for 2 h at 37°C in a humidified atmosphere. The tetrazolium salt was reduced to formazan by the succinate-tetrazolium reductase of the mitochondrial respiratory chain. The formazan dye produced by metabolically active cells was quantified with the use of a scanning multiwell spectrometer by measuring the absorbance of the dye solution at 450 and 620 nm. Experiments were carried out at least twice, with each experiment representing eight determinations. For each drug, the values included in the linear part of each experiment's sigmoid were retained in a linear regression analysis and were used to estimate the 50% inhibitory concentration (IC_{50}).

Live/Dead Fluorometric Assay

The live/dead fluorometric assay was performed according to the supplier's recommended protocol (Molecular Probes). Briefly, 10^6 HL-60 cells in exponential growth were treated with graded concentrations of drugs (0.01–1 μM) for 4 h before the flow cytometry analysis using Fl-1 (530 nm, log scale) for calcein-AM and Fl-3 (620 nm, linear scale) for ethidium homodimer-1 (EthD-1).

Cell Cycle Analysis

For flow-cytometry analysis of DNA content, 10^6 HL-60 cells in exponential growth were treated with 0.001 to 1 μM BN80915 or

SN38 for 4 h and then washed three times with citrate buffer. The cell pellet was incubated with 250 μl of trypsin-containing citrate buffer for 10 min at room temperature and then with 200 μl of citrate buffer containing a trypsin inhibitor and RNase (10 min) before adding 200 μl of propidium iodide at 125 μg/ml. Samples were analyzed with the use of a FACScan flow cytometer (BD Biosciences, San Jose, CA) using the Lysys II software, which is also used to determine the percentage of cells in the different phases of the cell cycle. Propidium iodide was excited at 488 nm, and fluorescence was analyzed at 620 nm (Fl-3).

BrdU Incorporation

Cells were cultured in complete RPMI 1640 medium with the test drug at 5 or 10 nM for 4 h before harvesting and then were pulse-labeled with 10 μM BrdU for 60 min in complete medium. After two washes in phosphate-buffered saline, pH 7.3, with sodium azide 0.1%, cells were fixed in ethanol 70% and incubated for 1 h at 4°C. After another wash in phosphate-buffered saline, cells were denatured in 2 N HCl for 15 min at 37°C (or for 30 min at room temperature) under gentle stirring. The pH was adjusted by a short incubation period (5 min) in 3 ml of 0.1 M $Na_2B_4O_7$, pH 8.5, before centrifugation (500*g* for 5 min at 4°C). The cell pellet was then washed with 5 ml of buffer containing PBS, Tween 0.05%, and 0.1% bovine serum albumin fraction V, resuspended in 50 μl of this buffer, and then incubated with the fluorescein isothiocyanate (FITC)-conjugated anti-BrdU monoclonal antibody (BD Biosciences) for 30 min at room temperature in the dark. For the negative controls, the pellet was incubated without the antibody. All cell pellets were washed with 1 ml of buffer containing PBS, Tween 0.05%, and 0.1% bovine serum albumin fraction V. Cells were collected by centrifugation, counterstained with 10 μg/ml propidium iodide, and treated with RNase (1 μg/ml). Samples were analyzed on a FACScan flow cytometer (BD Biosciences) using the Lysys II software.

Mitochondrial Membrane Potential ($\Delta\psi_{mt}$) Measurements

After the drug treatment (4 h at 37°C), 10^6 cells in 2 ml of complete RPMI 1640 medium were loaded with the probe $DiOC_6$ (50 nM) for 30 min at 37°C before flow cytometric analysis. The same incubation time was used for the controls and for the drug-treated samples. Control experiments were performed by incubating cells with CCCP (50 μM, 10 min at 37°C), a protonophore that abolishes $\Delta\Psi_{mt}$, and oligomycin (2.5 μg/ml, 10 min at 37°C), an uncoupling agent known to hyperpolarize mitochondrial membranes. $DiOC_6$ was excited at 488 nm, and fluorescence was analyzed at 525 nm (Fl-1) after logarithmic amplification. Forward scattering and side scattering images were analyzed after linear amplification. Similar experiments were performed with JC-1 (2 μg/ml). In this case, both the green (Fl-1) and red (Fl-3) fluorescences were recorded.

Intracellular pH

After the drug treatment, cells were pelleted and resuspended in 2 ml of Hanks' balanced salt solution before carboxy-SNARF-AM (0.1 μM) was added. After 1 h of incubation in a CO_2 incubator at 37°C, cells were pelleted, rinsed once with Hanks' balanced salt solution, and resuspended at an appropriate density for fluorescence measurements. The fluorescence excitation was set up at 488 nm, and the emission was recorded at 575 and 620 nm. Intracellular pH was estimated by comparison of the mean ratio values (fluorescence at 575 nm divided by fluorescence at 620 nm) of a sample to a calibration curve established by incubation of SNARF-AM loaded cells in varied pH buffer in the presence of the proton ionophore nigericin.

Detection of Bcl-2 by Confocal Microscopy

HL-60 cells (10^6) were treated with the test drug for 4 h at 37°C and then pelleted by centrifugation (300*g* for 5 min at 4°C), washed with PBS, pH 7.4, and fixed with a 0.25% paraformaldehyde solution for 15 min at room temperature in the dark. After washing, the cells were made permeable with 70% methanol at 4°C for 60 min and then washed again with PBS. The FITC conjugate of Bcl-2 (or the isotype for negative controls, 10 μM) was added directly to the cell pellet and incubated for 30 min at 4°C in the dark. PBS (2 ml) containing 2% fetal bovine serum was then added. After a brief centrifugation, the cell pellet was resuspended in 150 μl of PBS, and 100 μl (25,000 cells) was used for centrifugation (500 rpm with a cytospin, 5 min) on a slide. A drop of antifade solution containing the nucleus-specific dye TOTO-3 (0.1 μM) was added, and the treated portion of the slide was covered with a glass coverslip. The fluorescence of the TOTO-3 dye and the FITC-labeled Bcl-2 protein were detected and localized by confocal microscopy using a Leica DMIRBE microscope controlled by a Leica TCS-NT workstation (Leica Microsystems, Bensheim, Germany) with a 63 $\times$ 1.32 numerical aperture oil objective equipped with a 75 mW argon-krypton laser line. The emission signal was observed through a dichroic mirror (DD488/568) followed by a filter set (band filter, 530/30; band pass 600/30). The optical sections were obtained in the *z*-axis and stored on the computer with a scanning mode.

DEVD-pNA and IETD-pNA Cleavage

N-Acetyl-Asp-Glu-Val-Asp-pNA (DEVD-pNA) and *N*-acetyl-Ile-Glu-Thr-Asp-pNA (IETD-pNA) cleavage activities were measured using the ApoAlert CPP32/caspase-3 and ApoAlert Caspase-8 assay kits (CLONTECH, Heidelberg, Germany) according to the recommended protocols. Briefly, 2×10^6 exponentially growing HL-60 cells in 2 ml of RPMI 1640 medium were treated with the test drug at the indicated concentration for 4 h at 37°C. Cells were formed into pellets by centrifugation and resuspended in 50 μl of the lysis buffer. The lysed cell mixture was then incubated on ice for 10 min before centrifugation (12,000 rpm for 3 min at 4°C). Fifty microliters of 2$\times$ reaction buffer supplemented with 10 mM dithiothreitol was then added to each tube incubated at 4°C. During this period, a control was prepared by adding 0.5 μl of 1 mM DEVD-fmk or z-IETD-fmk to a cell sample treated with 0.1 μM staurosporine. The substrate DEVD-pNA or IETD-pNA was added to all tubes (5 μl, 50 μM) and the samples were incubated for 1 h at 37°C. The formation of *p*-nitroanilide was measured at 405 nm using a Multiskan MS microtiter plate reader (Labsystem, Helsinki, Finland).

Western Blotting

Poly(ADP-Ribose) Polymerase (PARP) Cleavage. Briefly, 7×10^5 exponentially growing HL-60 cells in a serum-free RPMI medium were treated with the test drug at the indicated concentration for 4 h at 37°C. Cells were formed into pellets by centrifugation (300*g* at 4°C for 5 min) and resuspended in 3 ml of lysis buffer containing 25 mM PBS, 0.1 mM phenylmethylsulfonyl fluoride, and the protease inhibitors chymostatin, leupeptin, aprotinin, and pepstatin A (5 μg/ml each). After centrifugation, cells were suspended again in the loading buffer containing 50 mM Tris-HCl, pH 6.8, 15% sucrose, 2 mM EDTA, 3% SDS, and 0.01% bromphenol blue. The mixture was sonicated for 30 s at 4°C and then heated to 100°C for 3 min. For Western blotting, the cell lysates (30 μg of proteins) were fractionated on a 7.5% polyacrylamide gel containing 0.1% SDS and then transferred onto a Hybond-C nitrocellulose membranes (Amersham Pharmacia Biotech, Orsay, France) for 40 min at 0.8 mA/cm^2 using a semidry transfer system. Membranes were blocked with 10% nonfat milk in PBST (0.1% Tween-20, 25 mM phosphate buffer, pH 7.4) for 30 min followed by incubation for 30 min with anti-PARP monoclonal antibody (CLONTECH, Palo Alto, CA) (1:10,000 dilution in PBST supplemented with 1% nonfat milk). The blots were washed three times (5 min each in PBST) and incubated with a goat anti-mouse IgG conjugated to horseradish peroxidase (Amersham Pharmacia Biotech; 1:10,000 dilution in PBST containing 1% nonfat milk) for 30 min. After three successives washes with PBST, the Western blot chemiluminescence reagent NEL105 (PerkinElmer Life Science Products, Boston, MA) was used for the detection.

Caspase-8 Activation and Bcl-2 Expression. HL-60 cells (7×10^5) were treated with BN80915, SN38, and/or topotecan at the indicated concentrations for 4 h at 37°C. Cells were centrifuged at 4°C, and washed twice with phosphate-buffered saline (3 ml at 4°C). After centrifugation (300*g* at 4°C for 5 min), lysates were resuspended in 25 μl of boiling buffer containing 10 mM Tris-HCl, pH 7.4, 1 mM Na-vanadate, 1% SDS, 0.1 mM phenylmethylsulfonyl fluoride, and the protease inhibitors leupeptin (5 μg/ml), aprotinin (10 μg/ml), and pepstatin A (2.5 μg/ml). The mixture was incubated for 10 min at 4°C before adding 75 μl of the electrophoresis dye solution (15% sucrose, 50 mM Tris-Hcl, 2 mM EDTA, 3% SDS, and 0.01% bromphenol blue). Samples were passed through a 26-gauge needle to reduce the viscosity of the solutions and then heated to 100°C for 3 min. For Western blotting, the cell lysates (30 μg of proteins) were fractionated on a 12.5% polyacrylamide gel containing 0.1% SDS and then transferred onto a Hybond-C nitrocellulose membranes (Amersham Pharmacia Biotech) for 40 min at 0.8 mA/cm^2 using a semidry transfer system. Membranes were blocked with 10% nonfat milk in PBST for 1 h at room temperature (or overnight at 4°C) followed by incubation with a mouse monoclonal antibody directed against caspase-8 (1/1000; Immunotech, Marseille, France), bcl-2 (1/1000; Immunotech), or actin (1/1000; Oncogene Research Products, Merck Eurolabo, Fontenay-sous-bois, France). Antibodies were diluted in PBST containing 2% nonfat milk, and membranes were incubated for 4 h in the dark under gentle agitation. The blots were washed three times (15 min each with PBST) and incubated for 1 h with a sheep anti-mouse IgG conjugated to horseradish peroxidase (Amersham Pharmacia Biotech; 1:10,000 dilution in PBST containing 2% nonfat milk). After three successive washes (15 min each) with PBST, the Western blot chemiluminescence reagent (PerkinElmer) was used for detection.

DNA Fragmentation

HL-60 cells at a density of 5×10^5 cells/ml were treated with BN80915 for 4 h and then collected by centrifugation at 2500*g* for 5 min. The resultant cell pellet was resuspended in PBS buffer containing 5 mM $MgCl_2$ and lysed in 500 μl of Tris-EDTA buffer containing 0.1% SDS and proteinase K (1.5 mg/ml) overnight at 37°C. After two successive extractions with phenol/chloroform, the aqueous layer was transferred to a new centrifuge tube. The DNA was precipitated with ethanol, resuspended in water (100 μl), and treated with RNase A (100 μg/ml) for 2 h at 37°C. Electrophoresis was performed in 1% agarose gel in Tris-borate buffer at approximately 12 V/cm for approximately 4 h. After electrophoresis, the gel was stained with ethidium bromide (1 mg/ml), washed, and photographed under UV light.

Terminal Deoxynucleotidyl Transferase–Mediated dUTP Nick-End Labeling (TUNEL) Assay

The apoptosis detection system fluorescein (Promega, Charbonnières, France) was used according to the supplier's recommended protocol. Briefly, 1×10^6 cells were treated with BN80915 or SN38 for 4 h, and then 30,000 cells were collected and centrifuged (cytospin) at 500 rpm for 5 min. Cells were fixed by immersion in 3% ice-cold paraformaldehyde solution (3 g; 0.1 mM $CaCl_2$, 0.1 mM $MgCl_2$, 100 ml PBS, pH 7.4) for 25 min at 4°C. Fixed cells were washed twice with PBS and made permeable in PBS containing Triton X-100 for 5 min in ice. Slides were rinsed twice in PBS. Excess PBS was drained off, and 100 μl of equilibration buffer was added for 5 to 10 min at room temperature for a pre-equilibration. DNA strand breaks (3′OH ends of fragmented DNA) were labeled with fluorescein-12-dUTP by adding incubation buffer containing equilibration buffer (45 μl), nucleotide mix (5 μl), and terminal deoxynucleotidyl transferase (1 μl) (volumes for one slide). After incubation in the dark at 37°C for 1 h, slides were dipped into 2× standard saline citrate to stop the reaction. After two successive washes, propidium iodide (1 μg/ml) was added to stain all cells. Apoptotic cells were detected and localized by green fluorescence (FITC-12-dUTP) on a red background [propidium iodide (PI)] by confocal microscopy, as described above.

Externalization of Phosphatidylserines

Surface exposure of phosphatidylserine (PS) by apoptotic HL-60 cells was measured with the use of cytometry by adding annexin V-FITC to 10^6 cells per sample according to the manufacturer's specifications (ApopNexin apoptosis detection kit; Oncor, Appligene, Illkirch, France). Simultaneously, the cells were stained with propidium iodide. Excitation was set at 488 nm, and the emission filters used were 515 to 545 (green, FITC) and 600 nm (red, PI). Data analysis was performed by use of the standard Lysys II software (BD Biosciences).

Results

Identification of Apoptotic Cells. The first method we used to characterize the effect of the drugs on HL-60 cells was a double-labeling procedure with the fluorescent markers calcein-AM and EthD-1. This method is very convenient for identifying apoptotic cells in a heterogeneous population of HL-60 cells treated with a topoisomerase inhibitor (Kluza et al., 2000). Intracellular esterases can convert the virtually nonfluorescent cell-permeant calcein-AM into the intensely green fluorescent calcein in viable cells. In contrast, EthD-1 enters cells with damaged membranes and undergoes a 40-fold enhancement of fluorescence upon binding to DNA, thereby producing a bright red fluorescence in dead cells. Cells were treated with graded concentrations of BN80915 for 24 h and then loaded with calcein-AM and EthD-1 before analysis by flow cytometry (Fig. 2). The populations of live (calcein$^+$) and dead (EthD-1$^+$) cells can easily be differentiated; in addition, however, a third population corresponding to cells stained both with calcein and EthD-1 can be detected. This double-stained cell fraction represents 25% of the cells upon treatment with 10 nM BN80915 and reaches 64% with

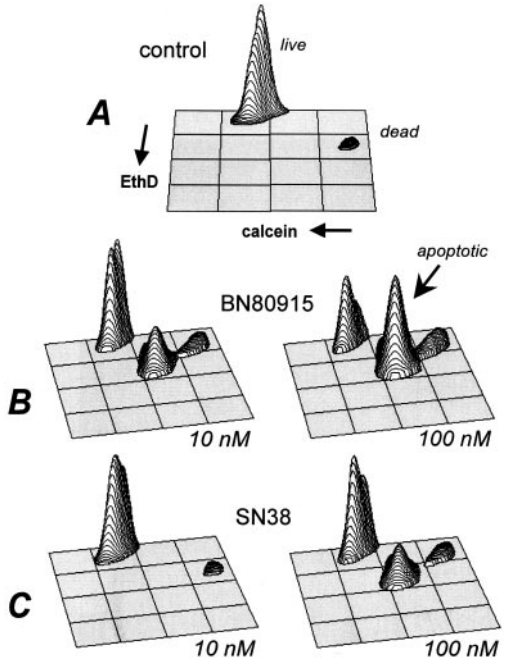

Fig. 2. Three-dimensional representation of the correlated distribution of calcein and EthD-1 fluorescence in HL-60 cells treated with 10 or 100 nM drug for 24 h.

100 nM drug. In comparison, these fractions represent only 0.5 and 21% of the cells treated with 10 nM and 100 nM SN38, respectively. We know from a previous study (Kluza et al., 2000) that these cells with an active metabolism (calcein$^+$) that allow EthD-1 to penetrate and stain their nucleic acids correspond to apoptotic cells, thus providing the first evidence that BN80915 also induces programmed cell death and that the effect was more pronounced than that of SN38.

Cell Cycle Effects. HL-60 cells were treated with increasing concentrations of the drugs for 4 h, and the DNA content was analyzed by cytometry after staining with propidium iodide (Fig. 3). In control cells, the G_1, S, and G_2+M populations represent 61, 18, and 16% of the cells, respectively. With this leukemia cell line, treatment with BN80915 or SN38 did not induce specific cell cycle arrest in the G_2+M phase, in contrast to other cell lines, such as P388, HT29, and B16 (data not shown). The drug treatment resulted in a loss of HL-60 cells in all three phases, of the cycle accompanied with a large increase in the subG1 region. Approximately 40 and 12% of the cells had DNA content less than G_1 after 4 h of treatment with 10 nM BN80915 and SN38, respectively. The subG1 population reaches 16 and 53% upon treatment with 50 nM BN80915 for 2 and 4 h, respectively. These drug-induced cell cycle perturbations concur with the results of the live/dead assay to suggest that myeloid leukemia HL-60 cells undergo apoptosis more extensively in the presence of BN80915 than with SN38. The cytometric, microscopic, and biochemical data reported below fully support this conclusion.

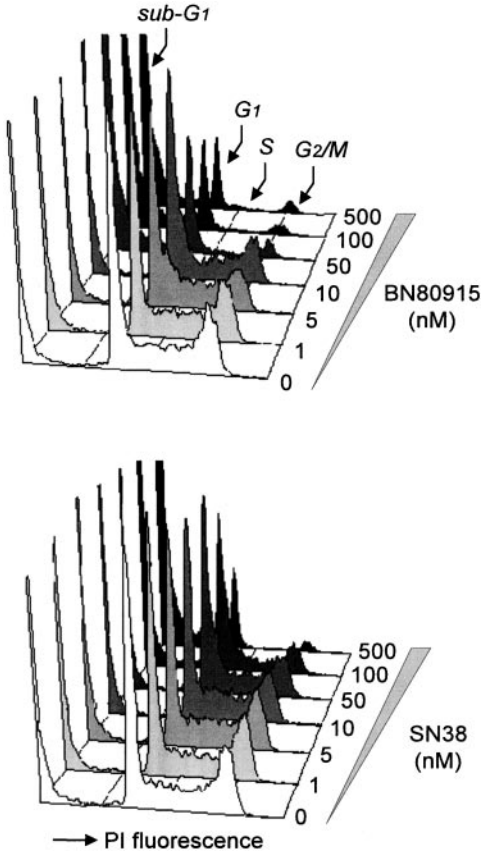

Fig. 3. Cell cycle analysis of HL-60 cells treated with graded concentrations of BN80915 and SN38 for 4 h. Cells were analyzed with the FACScan flow cytometer as described under *Materials and Methods*.

To get a more precise view of the drug effect at the S-phase level, cells were labeled with BrdU, a thymidine analog that incorporates into newly synthesized strands of DNA and can be used as a kinetic marker for cell proliferation. As shown in Fig. 4, fewer BrdU$^+$ cells, labeled in S-phase at the time of treatment, were detected after 4 h of treatment with BN80915 than in the control cell population. The decrease of the S-phase cell population resulting from the inhibition of BrdU incorporation into DNA was much more pronounced with the homocamptothecin derivative than with the conventional six-membered camptothecin drug. The potent inhibition of topoisomerase I and subsequent stimulation of DNA cleavage by drugs such as BN80915 and camptothecin reduce the entry of cells into the vulnerable DNA synthesis phase of the cell cycle.

Mitochondrial Membrane Potential ($\Delta\psi_{mt}$). The ampholytic cationic fluorescent probe $DiOC_6$ was used to monitor the drug-induced changes in the mitochondrial transmembrane potential ($\Delta\psi_{mt}$) (Zamzami et al., 2000). Cells were incubated with graded concentrations of BN80915 and SN38 (up to 500 nM) for 4 h, labeled with $DiOC_6$, and then analyzed by flow cytometry. In both cases, no significant variations of $\Delta\psi_{mt}$ were observed, whereas typical depolarization and hyperpolarization effects can be clearly detected with CCCP and oligomycin used as control probes (Fig. 5). Two additional mitochondria-specific fluorescent probes were used, mitotracker red and JC-1, but again no changes of $\Delta\psi_{mt}$ could be detected. We therefore concluded that in this cellular model, neither BN80915 nor SN38 affects the permeability of mitochondrial transition pores at the early stage of apoptosis.

pH Changes. To quantify the effect of the drugs on intracellular pH, HL-60 cells were loaded with the pH-sensitive dye carboxy-SNARF-AM, and the pH was determined in individual cells using ratiometric flow cytometry. The excitation was set at 488 nm, and the fluorescence emission was monitored at 575 and 620 nm. We observed that the intracellular pH decreases significantly upon treatment with both SN38 and BN80915. After 4 h of treatment with 0.05, 0.1, and 0.5 μM BN80915, the pH decreases from 7.32 to approximately 7.03, 6.82, and 6.55, respectively. The acidic shift was slightly less pronounced with SN38 (6.62 versus 6.55 at 0.5 μM).

Unchanged Bcl-2 Expression. Proteins of the Bcl-2 family play an important role in the cell death program induced

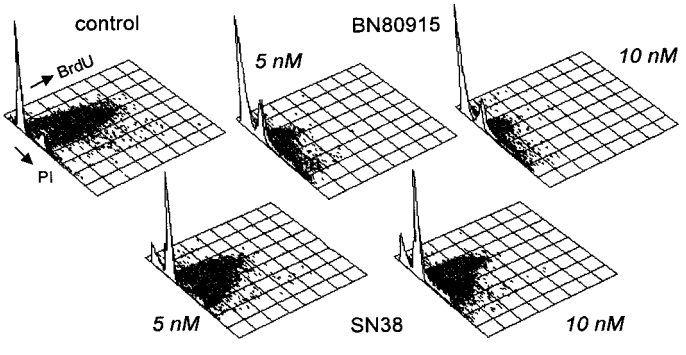

Fig. 4. Modification of bromodeoxyuridine incorporation in HL-60 cells treated with BN80915 and SN38. Cells were treated for 4 h with the test drug at 5 and 10 nM before labeling with the BrdU-FITC conjugate for 1 h.

by genotoxic drugs. In particular, the anti-apoptotic Bcl-2 protein acts at the mitochondrial level to prevent the release of apoptotic factors (e.g., cytochrome *c* and apoptosis-inducing factor) and activation of caspases (Antonsson and Martinou, 2000). Two complementary approaches were used to investigate the effect of the drugs on the expression of Bcl-2. Cells were immunostained with an anti-Bcl-2 antibody after the drug treatment and then observed by confocal microscopy. As shown in Fig. 6, cytoplasmic punctate distribution patterns were observed with both untreated (control) and drug-treated cells, be it with SN38 or BN80915. It is known that Bcl-2 localizes to the outer mitochondrial membrane but also to the endoplasmic reticulum and the nuclear membrane (Chen-Leavy and Cleary, 1990). The green fluorescence associated with the immunolabeled Bcl-2 protein is restricted to the cytoplasmic compartment, whereas the blue fluorescence of the dye TOTO-3 is found in the nucleus of the cells. Both drug concentrations and time of incubation were varied, but in all cases, no significant changes of the level of green fluorescence in the cytoplasm of HL-60 were detected for cells treated with BN80915 or SN38. In parallel, Bcl-2 was detected by Western blot analysis, and again we found no variation in the expression of the protein for either SN38 or BN80915 (Fig. 6).

Caspases Activation. Three complementary experimental approaches were used to determine whether caspases participate in the propagation of apoptosis induced by BN80915 in the human HL-60 cell line. First, lysates from drug-treated cells were assayed for the cleavage of the *p*-nitroaniline–tagged peptides DEVD-pNA and IETD-pNA, which represent preferential substrates for caspase-3 and -8, respectively. In these solution assays, caspase activation leads to the release of pNA, which can be easily monitored by absorbance measurements at 405 nm using a 96-well plate reader. With both substrates, pronounced peptidase activities were detected (Fig. 7, a and b). Much lower concentrations of BN80915 than SN38 were required to detect the scission of the two synthetic peptide substrates. For example, at 0.02 μM, the homocamptothecin derivative fully activated the two caspases, whereas a 10-fold higher concentration of the camptothecin derivative was required to induce a similar extent of peptide cleavage mediated by the caspases. With the IETD-pNA substrate, the absorbance measured after treatment of the cells with 0.2 μM SN38 for 4 h was only marginally higher than that measured in the control (drug-free) lysates (Fig. 7d). In contrast, the effect of BN80915 was pronounced and comparable with that measured with the positive control drugs such as the protein kinase C inhibitor staurosporine, a potent inducer of apoptosis. The caspase-mediated cleavage activity stimulated by BN80915 or SN38 was totally inhibited by the inhibitors z-DEVD-fmk or z-IETD-fmk (Fig. 7, c and d). The activation of caspases was also clearly evident from cytometry experiments using a FITC conjugate of the caspase inhibitor valyl-alanyl-aspartyl-[*O*-methyl]-fluoromethylketone (CaspACE *in situ* marker, Promega). This cell-permeable compound binds irreversibly to activated caspases. Upon treatment of the cells with 0.1 μM SN38 or BN80915 for 4 h, an intense fluorescence was recorded with the cells exposed to the drugs but not with the untreated control sample (data not shown).

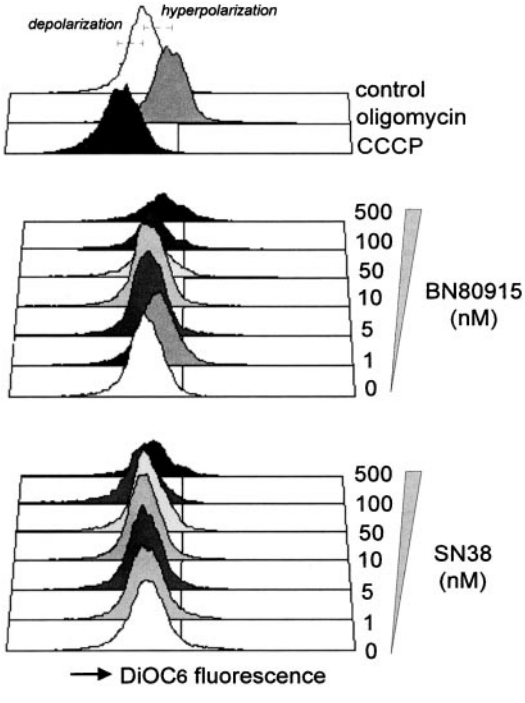

Fig. 5. Effect of the drugs on the mitochondrial membrane potential ($\Delta\psi_{mt}$). The cytofluorometric profiles show the variations of the fluorescence of the $\Delta\Psi_{mt}$-sensitive dye $DiOC_6$ after exposure of HL-60 cells for 4 h with graded concentrations of BN80915 or SN38 (up to 500 nM). The two drugs do not affect $\Delta\psi_{mt}$, whereas the control probes oligomycin (1.25 μg/ml, 10 min at 37°C) and CCCP (50 μM, 10 min at 37°C) induce hyperpolarization and depolarization, respectively. Cells were stained with 50 nM $DiOC_6$ before analysis by flow cytometry.

Next, we examined the cleavage of PARP, an enzyme involved in DNA repair that is a good substrate for caspase-3. PARP catalyzes the transfer of the ADP ribose moiety from NAD^+ to a limited number of protein acceptors involved in chromatin architecture or in DNA metabolism, including topoisomerase I. The two Western blots presented in Fig. 8 show that the native 116-kDa PARP protein was cleaved into its characteristic 89-kDa fragment upon treatment of the cells with the drugs. The 24-kDa fragment could not be detected because the anti-PARP antibody recognizes only the COOH terminus of the protein. Here again, the homocamptothecin derivative BN80915 proved significantly more potent than SN38 at stimulating the cleavage of the target protein. For example, 0.05 and 0.1 μM BN80915 induced 51 and 60% cleavage of PARP, respectively, whereas SN38 induced only 10 and 31% cleavage, respectively, at the same concentrations. The cleavage of PARP was detected after 3 h of treatment with BN80915 (Fig. 8, bottom).

In parallel, a similar Western blot procedure was performed to follow the proteolytic activation of the intracellular levels of caspase-8 in HL-60 cells. Caspase-8 is synthesized as two isoforms of ~55 kDa. The immunoblot shown in Fig. 9 reveals that 0.1 μM BN80915 induced approximately 26% cleavage of procaspase-8, whereas at the same concentration, both SN38 and topotecan (TPT) showed almost no effect on the cleavage of the protein. At 1 μM, BN80915, SN38, and TPT induced 38, 22, and 28% cleavage of procaspase-8, respectively. Therefore, the activation of caspases-3 and -8 shown by the Western blot experiments fully agree with the colorimetric assay using DEVD- and IETD-pNA peptide substrates. From these two sets of experiments, we conclude that BN80915 strongly activates both the initiator caspase-8 and the effector caspase-3.

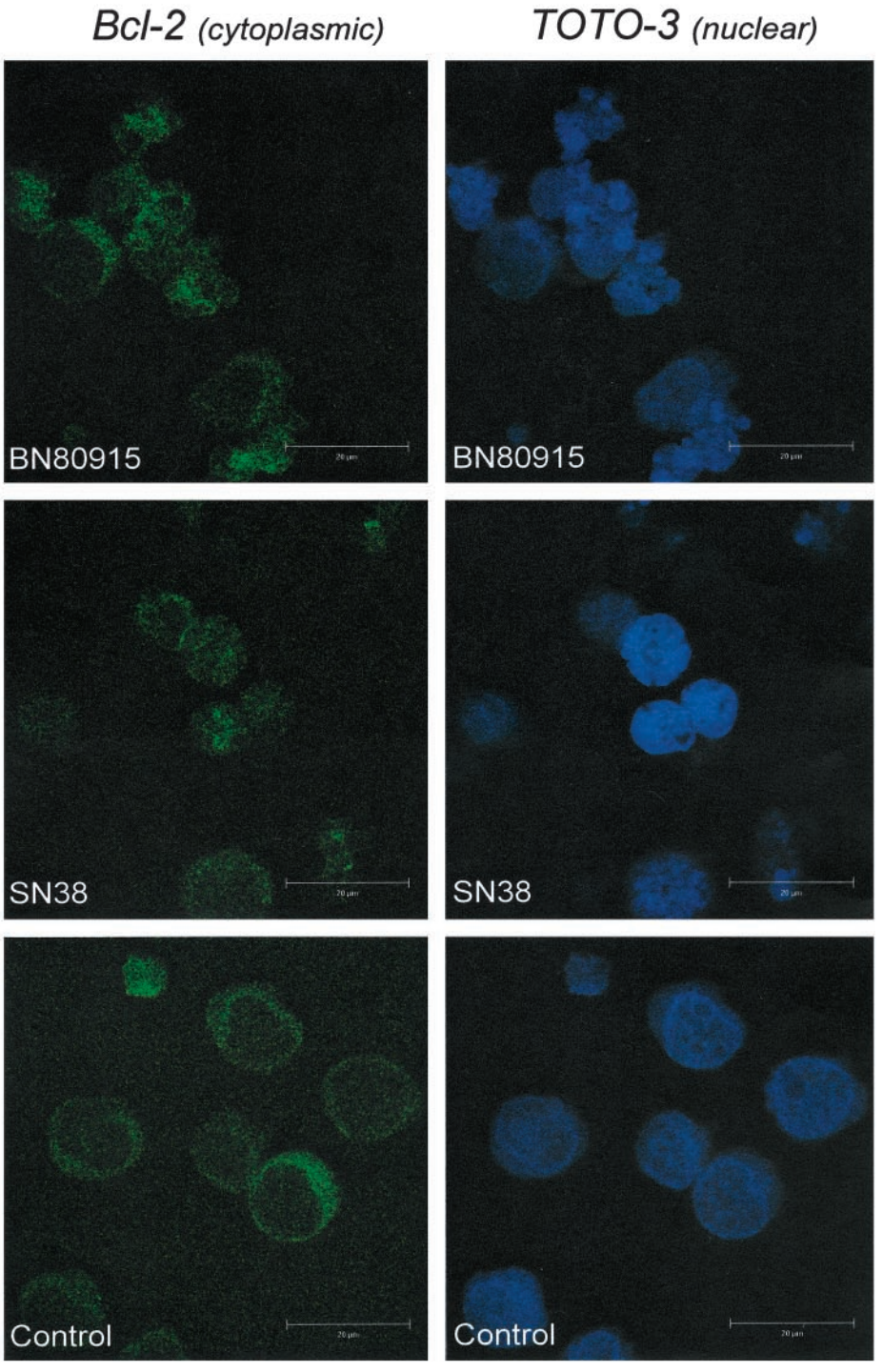

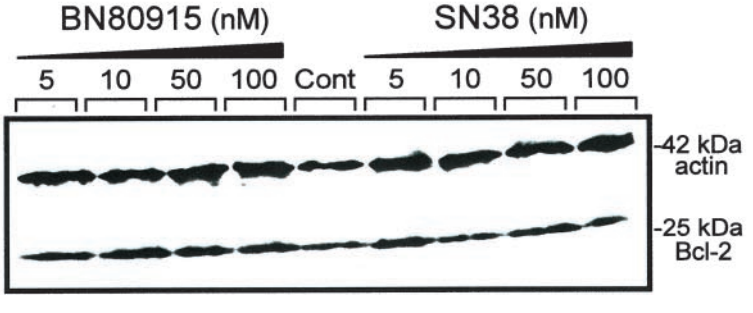

Fig. 6. Laser scanning confocal microscopy of Bcl-2 expression in untreated HL-60 cells (control) and cells treated for 4 h with 0.1 μM BN80915 or SN38. After fixation/permeabilization, cells were processed for Bcl-2 labeling using a FITC-coupled monoclonal antibody (green). At the same time, cells were stained with the nuclear-specific TOTO-3 dye before examination under a confocal laser-scanning microscope. The Western blot below the figures shows the expression of Bcl-2 in untreated HL-60 cells (control) and cells treated for 4 h with increasing concentrations of SN38 or BN80915. Cell proteins were subjected to SDS-PAGE followed by blotting with an anti-Bcl-2 monoclonal antibody. The 25-kDa band refers to Bcl-2 and the 42-kDa band refers to actin, which was detected with an anti-actin monoclonal antibody to confirm the equal amount of protein in each lane.

DNA Fragmentation. The DNA of HL-60 cells treated for 4 h with BN80915 or SN38 was extracted and analyzed by native agarose gel electrophoresis. Untreated cells contained only high-molecular-weight genomic DNA, whereas both drugs produced DNA fragments of lower molecular weight consisting of multimers of 180 base pairs. An example of DNA ladder obtained with BN80915 is shown in Fig. 10. The drug-induced DNA strand breaks were characterized further using the TUNEL assay, because of the fluorescein-labeling of apoptotic DNA fragments in situ. The fluorescence intensity profiles in Fig. 10 show the distribution of FITC and PI fluorescence along the *xy*-axis indicated on the photographs. These two plots attest that BN80915 induces more DNA strand breaks than SN38. With this method, DNA strand breaks occurring before the nuclear fragmentation can be detected (Kaufmann et al., 2000). Cells were treated with the drugs at 0.1 μM for 4 h, stained, and then analyzed by confocal microscopy. As shown in Fig. 10, control cells containing intact genomic DNA were shown in red (because of the staining with propidium iodide), whereas apoptotic cells containing multiple DNA breaks were shown in yellow. The analysis of many different slides revealed that not only was the number of TUNEL$^+$ cells approximately 30% higher with BN80915 than with SN38, but also the yellow staining was generally more pronounced in apoptotic cells treated with the homocamptothecin than with the benchmark compound.

Externalization of Phosphatidylserines. PS lipids are normally confined to the inner leaflet of the plasma membrane but become exported to the outer face during apoptosis and serve as a trigger for recognition of apoptotic cells by phagocytes. PS can be detected by staining with a FITC conjugate of annexin V, a 38 kDa anticoagulant protein that binds naturally to PS (Bossy-Wetzel and Green, 2000). The cells were treated with 10 and 50 nM SN38 or BN80915 for 4 h or 24 h before monitoring binding of annexin V by flow cytometry. After 4 h of drug treatment, we detected very little annexin$^+$ HL-60 cells. This observation is consistent with results from a previous study showing that HL-60 cells treated with 300 nM camptothecin for 4 h caused no detectable increase in annexin V

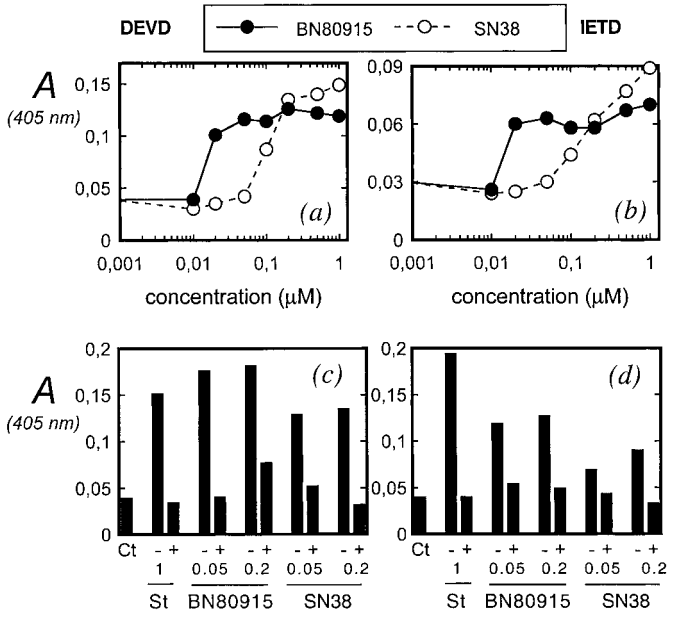

Fig. 7. Evaluation of DEVD- and IETD-dependent cleavage activities. HL-60 cells were incubated with BN80915 or SN38 at the indicated concentration for 4 h before adding the caspase-3 substrate DEVD-pNA (a, c) or the caspase-8 substrate IETD-pNA (50 μM) (b, d). The histograms show the DEVDase (c) and IETDase (d) activities without drug (control, Ct), in the presence of 0.1 μM staurosporine (St), and 0.05 or 0.2 μM BN80915 or SN38, in the absence (−) or presence (+) of a caspase inhibitor z-DEVD-fmk or z-IETD-fmk (10 μM). Results are the mean of three experiments.

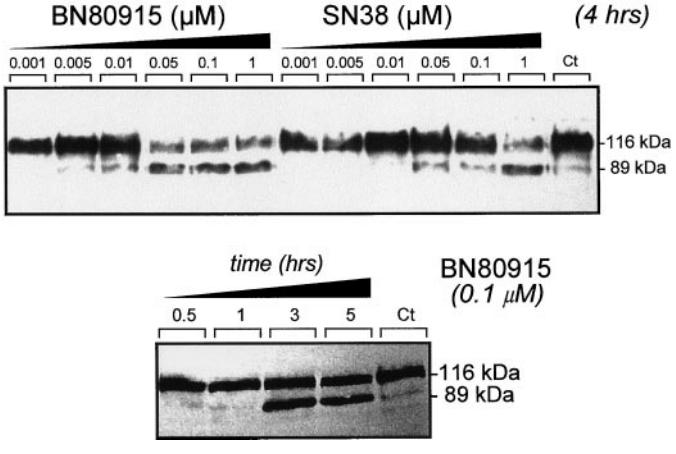

Fig. 8. Western blot analysis for the cleavage of PARP. Control lanes (Ct) refer to untreated cells. In the other lanes, the cells were treated with BN80915 or SN38 at the indicated concentration (μM) for 4 h before the Western blot analysis. Bottom, the result of a time course experiment with cells exposed to 0.1 μM BN80915 for 0.5 to 5 h. In all cases, whole cell lysates and equal amount of proteins in each lane were subjected to SDS-PAGE followed by blotting with an anti-PARP monoclonal antibody. The molecular masses of the full-length protein and its cleavage fragment are indicated.

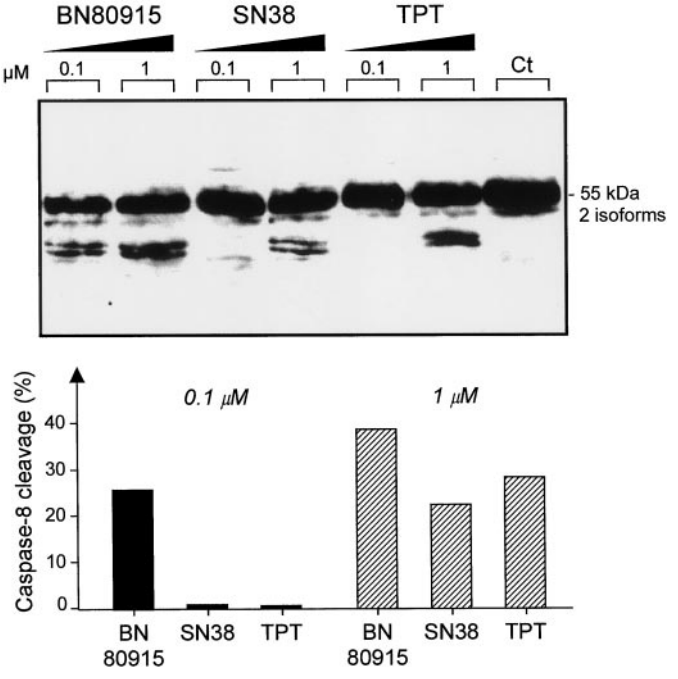

Fig. 9. Western blot analysis for the activation of caspase-8. Cells were treated with 0.1 or 1 μM BN80915, SN38, or topotecan TPT for 4 h before the Western blot analysis. The lane marked Ct refers to untreated cells. Cell proteins were subjected to SDS-PAGE followed by blotting with an anti-caspase-8 monoclonal antibody. The histogram shows the extent of cleavage of caspase-8 determined after densitometric analysis of three gels, as shown in the figure.

binding (Frey, 1997). After a 24 h period, PS became exposed on the outside of the cell plasma membranes, as judged from the massive labeling with the annexin V-FITC conjugate. As shown in Fig. 11, much higher levels of HL-60 cells stained positively for FITC-labeled annexin V upon treatment with BN80915 than with SN38. The data confirm the idea that, in HL-60 cells, the apoptotic process of DNA cleavage precedes externalization of PS residues. King et al. (2000) have recently shown that there is substantial nuclear and cellular disintegration before detectable PS exposure during camptothecin-induced apoptosis of HL-60 cells.

Cell Viability. A tetrazolium-based assay (WST1) was used to compare the effects of BN80915 and SN38 on cell viability. HL-60 cells were treated with graded concentrations of the two compounds for 4 h and then cultivated for a subsequent period, up to 72 h, in a drug-free medium before evaluating the cytotoxicity. After a short exposure to the drugs followed by 3 days of culture in a drug-free medium, BN80915 seemed two times more toxic than SN38 (IC_{50}

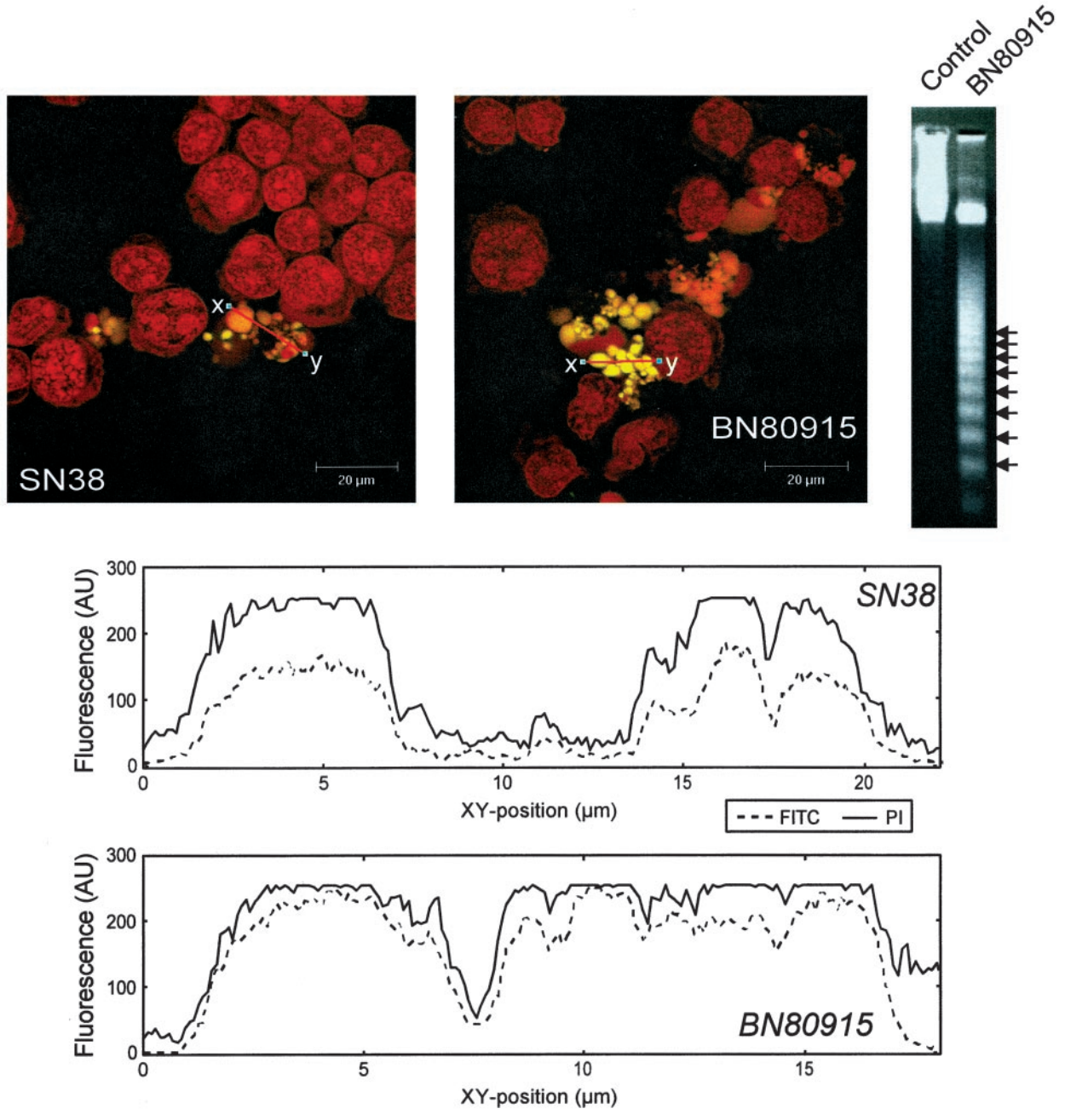

Fig. 10. Effects of BN80915 and SN38 on DNA fragmentation. HL-60 cells were treated with the drugs at 0.1 μM for 4 h before analysis of DNA integrity by the TUNEL technique and confocal microscopy or by agarose gel electrophoresis. The two photographs show TUNEL$^+$ cells stained in yellow and nonapoptotic cells stained in red with propidium iodide. The graphs show the distribution of the FITC and PI fluorescence along the *xy*-axis indicated in the photographs for both SN38 and BN80915. Top right, a typical agarose gel electrophoresis of DNA extracted from untreated HL-60 cells (control) and cells treated with 0.1 μM BN80915 for 4 h. DNA was stained with ethidium bromide after electrophoresis on a 1% agarose gel and then visualized under UV light. Internucleosomal DNA fragmentation can be clearly seen in drug-treated cells (arrows).

values after 72 h were 0.17 and 0.34 μM for BN80915 and SN38, respectively). The two drugs showed comparable toxicity when the cell culture was maintained for only 24 h (IC_{50} values after 24 h were 1.31 and 2.0 μM for BN80915 and SN38, respectively). However, it must be kept in mind that this type of assay is based on the reduction of a tetrazolium salt into a colored formazan dye by mitochondrial dehydrogenases. Therefore, it is likely that intact cells and apoptotic cells with active mitochondrial functions show similar responses in this assay.

Discussion

Recent studies have shown that the homocamptothecin derivative BN80915 produces more DNA strand breaks in vitro than SN38 and stimulates DNA cleavage at more sites than the benchmark product SN38 (Demarquay et al., 2001; Larsen et al., 2001). BN80915 is one of the most potent topoisomerase I inhibitors described. Indeed, the drug exhibits remarkable antitumor activity against xenografted tumors in mice and has recently entered phase I clinical trials.

The multiple DNA strand breaks induced by BN80915 trigger induction of the apoptosis program in HL-60 cells. Exactly how the cell death program is engaged after topoisomerase I inhibition remains unclear. We have demonstrated that BN80915 is a potent inducer of apoptosis in HL-60 cells. This induction of apoptosis is associated with (1) cell cycle changes, (2) a marked decrease of intracellular pH, (3) activation of caspase-3 and -8, (4) DNA fragmentation, and (5) externalization of phosphatidylserine lipids but no significant changes of the mitochondrial membrane potential or the expression of Bcl-2. These different events are interconnected. The accumulation of topoisomerase I-mediated DNA strand breaks can cause the failure of DNA repair and subsequent arrest of the cell cycle during the S-phase. We envision the poisoning of topoisomerase I as the signal triggering mitochondrial activation. However, further investigations are needed to identify the signal(s), downstream of topoisomerase I and upstream of mitochondria, involved in activation of the apoptosis machinery. Identification of these specific targets may have profound therapeutic implications. Two putative key components in the transfer of the initial signal (e.g., DNA damages) from the nucleus to mitochondria are the transcription factors p53 and TR3. The protein p53 was recently shown to migrate from the nucleus to the mitochondria, in which it interacts with the heat shock protein hsp70 (Marchenko et al., 2000). In our case, this transport process is most unlikely because HL-60 cells are p53-null (Wolf and Rotter, 1985). In the same context, a very recent study showed that the protein TR3—an orphan member of the steroid-thyroid hormone-retinoid receptor superfamily of transcription factors—can also translocate from the nuclear compartment to mitochondria, in which it triggers membrane permeability, cytochrome *c* release, and apoptotic cell death (Li et al., 2000a). Many different apoptotic stimuli can induce mitochondrial targeting of TR3, including the antitumor drug etoposide, which is a powerful topoisomerase II inhibitor (Li et al., 2000b). We believe that this potential transport process is unlikely to occur in our case because BN80915 does not induce significant changes of $\Delta\psi_{mt}$, suggesting that the drug has little effect on the permeability of the mitochondrial membrane. We have recently reported that the tumor-active topoisomerase II poisons TAS-103 (Kluza et al., 2000) and etoposide (Facompré et al., 2000) both induce profound changes of $\Delta\psi_{mt}$ and that the variations of the membrane potential are correlated with the cell cycle changes in HL-60 cells. With both drugs, the accumulation of cells in the G_2/M phase was accompanied by an increase of $\Delta\psi_{mt}$ (hyperpolarization), whereas the subsequent decrease of the G_2/M population was detected simultaneously with the decrease of $\Delta\psi_{mt}$ (depolarization). Here we show that with the same cell line, the topoisomerase I poison BN80915 neither provokes a G_2/M arrest nor affects the mitochondrial membrane potential. Nevertheless, BN80915 triggers massive apoptosis in HL-60 cells. The lack of variation of $\Delta\psi_{mt}$ upon treatment with BN80915 and SN38 was observed with HL-60 cells as well as with HT29 colon carcinoma, P388 leukemia, and B16 melanoma cells treated with 100 nM SN38 or BN80915 (data not shown). Therefore, it seems that HL-60 cells do not represent a special case for the action of (homo)camptothecins, but in a recent study with the Jurkat cell line, significant variations of $\Delta\psi_{mt}$ were observed upon treatment with camptothecin, and the changes of the mitochondrial membrane potential were connected with variations of the cytochrome *c* level (Sánchez-Alcázar et al., 2000). However, in another recent study with HL-60 cells induced with camptothecin (Li et al., 2000b), no dissipation of $\Delta\psi_{mt}$ was observed, in agreement with the data reported here.

The lack of dissipation of $\Delta\psi_{mt}$ prompted us to investigate the effect of the drug on the expression level of the antiapoptotic Bcl-2 protein, which has been shown to stabilize $\Delta\psi_{mt}$ (Desagher and Martinou, 2000) and play an important role in apoptosis (Makin and Hickman, 2000). The mechanism by which Bcl-2 and related proteins oppose apoptosis may involve prevention of mitochondrial damages (e.g., loss of $\Delta\psi_{mt}$) (Marchetti et al., 1996). According to the confocal microscopy and Western blot data presented in Fig. 6, the expression level of the antiapoptotic Bcl-2 protein is not significantly affected by the drugs, but this does not mean that this protein plays no role in the drug-induced apoptotic process. The expression level can remain constant while the protein activity varies considerably. Recent studies on the related proapoptotic proteins Bax and Bak have revealed that important conformational changes of the protein occur during apoptosis progression, and each conformation may act as a regulator of the apoptotic machinery (Griffiths et al., 1999; Taylor et al., 2000). Interaction of Bcl-2 with related

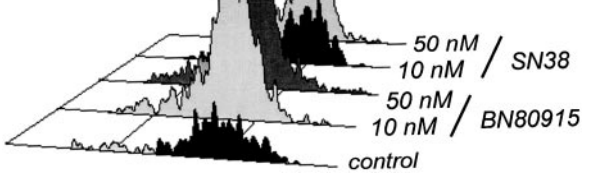

Fig. 11. Drug-induced externalization of phosphatidylserine residues. Untreated HL-60 cells (control) and cells treated with 10 or 50 nM BN80915 or SN38 for 24 h were subsequently stained with an annexin V-FITC conjugate specifically detecting the exposure of PS residues at the cell surface.

(e.g., Bax) or unrelated proteins (e.g., RAD-9) involved in the control of a cell cycle checkpoint (Komatsu et al., 2000), as well as post-translational modification by phosphorylation, can also modulate the activity of the protein (Haldar et al., 1995). Phosphorylation of Bcl-2 can antagonize the ability of this protein to block mitochondrial dysfunction and apoptosis (Uhlmann et al., 1996). However, the impact of this process probably varies with the cell type and/or the inciting apoptotic stimulus because conflicting results have been reported in the literature to define the role of Bcl-2 phosphorylation in regulation of apoptosis (Tang et al., 2000).

Drug-induced intracellular acidification is expected to modulate caspase activation during apoptosis. For example, activation of cytosolic caspases by cytochrome *c* is minimal at neutral pH but maximal at acidic pH (Matsuyama et al., 2000). We have shown that both caspase-3 and -8 are activated by BN80915. The proximal caspase-8 can directly activate the distal caspase-3 (Stennicke et al., 1998), but there are probably many other similar proteases involved in the full apoptotic program. Several studies with topoisomerase I inhibitors have shown that programmed cell death is associated with activation of a number of these aspartate-specific cysteine proteases (Shimizu and Pommier, 1997). The activation of caspase-3 and -8 could be responsible for the externalization of phosphatidylserine residues because the appearance of outer leaflet PS requires caspase activation. Similarly, the degradation of DNA in either large pieces or small oligonucleosomal fragments may be a late consequence of the activation of endonucleases by caspases (Degen et al., 2000) and/or the release from mitochondria of nuclease-activating proteins, such as the apoptosis-inducing factor (Daugas et al., 2000). Two types of deoxyribonuclease activities have been detected during apoptotic death: one that generates 30- to 500-kilobase pair domain-sized fragments, and another that mediates internucleosomal DNA degradation (Robertson and Zhivotovsky, 2000). At least the former type of DNases is recruited by BN80915 to produce DNA breakage *en masse* in HL-60 cells.

Collectively, the data reported here show that the highly potent topoisomerase I poison BN80915 is a powerful pro-apoptotic agent. This homocamptothecin derivative, currently subjected to clinical testing, induces apoptosis in HL-60 cells more potently than the benchmark drug SN38, presumably as a result of its higher topoisomerase I poisoning capacity. The molecular pathway leading to apoptotic cell death with BN80915 is different from that observed with topoisomerase II poisons such as TAS-103 and etoposide (at least with the HL-60 cell line), although characteristics such as activation of caspases and DNA fragmentation are observed. The promyelocytic HL-60 cell lines have been used extensively to study drug-induced apoptosis, particularly with camptothecin (Palissot et al., 1996; Shimizu and Pommier, 1997; King et al., 2000).

This study provides a better understanding of the mechanism of action of BN80915. In particular, it helps to illustrate how the cell death program is engaged after topoisomerase I inhibition by the homocamptothecin derivative. We show that nucleases and caspases probably represent key actors of the BN80915-induced cell death process. Many other signaling molecules, particularly kinases and phosphatases (Utz and Anderson, 2000), as well as heat shock proteins, should also play a critical role in the execution phase of apoptosis induced by BN80915. There are a vast number of signaling molecules involved in the transduction of the initial cell death stimulus from the nucleus to mitochondria or other nodal points in the target cells (Solary et al., 2000). The number of effector molecules involved in the apoptotic cascade is growing fast, and characterization of all these "sensors" will require appropriate technologies. Further studies to answer this question are in progress.

References

Antonsson B and Martinou JC (2000) The Bcl-2 protein family. *Exp Cell Res* **256:** 50–57.

Bailly C, Laine W, Baldeyrou B, Demarquay D, Huchet M, Coulomb H, Lanco C, Lavergne O and Bigg DCH (2001) A novel B-ring modified homocamptothecin, 12-Cl-hCPT, showing antiproliferative and topoisomerase I inhibitory activities superior to SN-38. *Anticancer Drug Des*, in press.

Bailly C, Lansiaux A, Dassonneville L, Demarquay D, Coulomb H, Huchet M, Lavergne O and Bigg DCH (1999) Homocamptothecin, an E-ring modified camptothecin analog, generates new topoisomerase I-mediated DNA breaks. *Biochemistry* **38:**15556–15563.

Bom D, Curran DP, Chavan AJ, Kruszewski S, Zimmer SG, Fraley KA and Burke TG (1999) Novel A, B, E-Ring-modified camptothecins displaying high lipophilicity and markedly improved human blood stabilities. *J Med Chem* **42:**3018–3022.

Bossy-Wetzel E and Green DR (2000) Detection of apoptosis by annexin V labeling. *Methods Enzymol* **322:**15–18.

Chen-Leavy S and Cleary ML (1990) Membrane topology of the Bcl-2 proto-oncogenic protein demonstrated in vitro. *J Biol Chem* **265:**4929–4933.

Daugas E, Nochy D, Ravagnan L, Loeffler M, Susin SA, Zamzami N and Kroemer G (2000) Apoptosis-inducing factor (AIF) a ubiquitous mitochondrial oxidoreductase involved in apoptosis. *FEBS Lett* **476:**118–123.

Degen WGJ, Pruijn GJM, Raats JMH and van Venrooij WJ (2000) Caspase-dependent cleavage of nucleic acids. *Cell Death Differ* **7:**616–627.

Demarquay D, Huchet M, Coulomb H, Lesueur-Ginot L, Lavergne O, Kasprzyk PG, Bailly C, Camara J and Bigg DCH (2001) The homocamptothecin BN80915 is a highly potent orally active topoisomerase I poison. *Anticancer Drugs* **12:**9–19.

Desagher S and Martinou JC (2000) Mitochondria as the central control point of apoptosis. *Trends Cell Biol* **10:**369–377.

Facompré M, Wattez N, Kluza J, Lansiaux A and Bailly C (2000) Relationship between cell cycle changes and variations of the mitochondrial membrane potential induced by etoposide. *Mol Cell Biol Res Commun* **4:**37–42.

Frey T (1997) Correlated flow cytometric analysis of terminal events in apoptosis reveals the absence of some changes in some model systems. *Cytometry* **28:**253–263.

Griffiths GJ, Dubrez L, Jones NH, Morgan CP, Whitehouse J, Corfe BM, Dive C and Hickman JA (1999) Cell damage-induced conformational changes of the pro-apoptotic protein Bak in vivo precede the onset of apoptosis. *J Cell Biol* **144:**903–914.

Haldar S, Jena N and Croce CM (1995) Inactivation of Bcl-2 by phosphorylation. *Proc Natl Acad Sci USA* **92:**4507–4511.

Kaufmann SH, Mesner PW Jr, Samejima K, Tone S and Earnshaw WC (2000) Detection of DNA cleavage in apoptotic cells. *Methods Enzymol* **322:**3–15.

King MA, Radicchi MA and Wells JV (2000) There is substantial nuclear and cellular disintegration before detectable phosphatidylserine exposure during the camptothecin-induced apoptosis of HL-60 cells. *Cytometry* **40:**10–18.

Kluza J, Lansiaux A, Wattez N, Mahieu C, Osheroff N and Bailly C (2000) Apoptotic response of HL-60 human leukemia cells to the antitumor drug TAS-103. *Cancer Res* **60:**4077–4084.

Komatsu K, Miyashita T, Hang H, Hopkins KM, Zheng W, Cuddeback S, Yamada M, Lieberman HB and Wang HG (2000) Human homologue of S. pombe Rad9 interacts with Bcl-2/Bcl-xL and promotes apoptosis. *Nat Cell Biol* **2:**1–6.

Larsen AK, Gilbert C, Chyzak G, Plisov SY, Naguibneva I, Lavergne O, Lesueur-Ginot L and Bigg DCH (2001) Unusual potency of BN 80915, a novel fluorinated E-ring modified camptothecin, toward human colon carcinoma cells. *Cancer Res* **61:**2961–2967.

Lavergne O, Demarquay D, Bailly C, Lanco C, Rolland A, Huchet M, Coulomb H, Muller N, Baroggi N, Camara J, et al. (2000) Preparation and in vitro activity of enantiomerically pure, fluorinated homocamptothecins as potent topoisomerase I poisons. *J Med Chem* **43:**2285–2289.

Lavergne O, Lesueur-Ginot L, Pla Rodas F and Bigg DCH (1997) BN80245: an E-ring modified camptothecin with potent antiproliferative and topoisomerase I inhibitory activities. *Bioorg Med Chem* **7:**2235–2238.

Lavergne O, Lesueur-Ginot L, Pla Rodas F, Kasprzyk G, Pommier J, Demarquay D, Prevost G, Ulibarri G, Rolland A, Schiano-Liberatore AM, et al. (1998) Homocamptothecins: synthesis and antitumor activity of novel E-ring-modified camptothecin analogues. *J Med Chem* **41:**5410–5419.

Lesueur-Ginot L, Demarquay D, Kiss R, Kasprzyk PG, Dassonneville L, Bailly C, Camara J, Lavergne O and Bigg DCH (1999) Homocamptothecin, an E-ring modified camptothecin with enhanced lactone stability, retains topoisomerase I-targeted activity and antitumor properties. *Cancer Res* **59:**2939–2943.

Li H, Kolluri SK, Gu J, Dawson MI, Cao X, Hobbs PD, Lin B, Chen G, Lu JF, Xie Z, et al. (2000a) Cytochrome c release and apoptosis induced by mitochondrial targeting of nuclear orphan receptor TR3. *Science (Wash DC)* **289:**1159–1164.

Li X, Du L and Darzynkiewicz Z (2000b) During apoptosis of HL-60 and U-937 cells caspases are activated independently of dissipation of mitochondrial electrochemical potential. *Exp Cell Res* **257:**290–297.

Makin G and Hickman JA (2000) Apoptosis and cancer chemotherapy. *Cell Tissue Res* **301:**143–152.
Marchenko ND, Zaika A and Moll UM (2000) Death signal-induced localization of pR3 protein to mitochondria. *J Biol Chem* **275:**16202–16212.
Marchetti P, Castedo M, Susin SA, Zamzami N, Hirsch T, Machio A, Haeffner A, Hirsch F, Geuskens M and Kroemer G (1996) Mitochondrial permeability transition is a central coordinating event of apoptosis. *J Exp Med* **184:**1155–1160.
Matsuyama S, Llopis J, Deveraux QL, Tsien RY and Reed JC (2000) Changes in intramitochondrial and cytosolic pH: early events that modulate caspase activation during apoptosis. *Nat Cell Biol* **2:**318–325.
Palissot V, Liautaud-Roger F, Carpentier Y and Dufer J (1996) Image cytometry of early nuclear events during apoptosis induced by camptothecin in HL-60 leukemic cells. *Cytometry* **25:**341–348.
Philippart P, Harper L, Chaboteaux C, Decaestecker C, Bronckart Y, Gordover L, Lesueur-Ginot L, Malonne H, Lavergne O, Bigg DCH, et al. (2000) Homocamptothecin, an E-ring-modified camptothecin, exerts more potent antiproliferative activity than other topoisomerase I inhibitors in human colon cancers obtained from surgery and maintained in vitro under histotypical culture conditions. *Clin Cancer Res* **6:**1557–1562.
Principe P, Marsais J, Kasprzyk PG, Carlson M, Lauer J, Meshaw K, Alford TL, Hill B, Chen SF, Hollister BA, et al. (1999) Anti-tumour profile of BN80915, a novel E-ring modified topoisomerase I inhibitor (Abstract 664). *Clin Cancer Res* **5:**3862s.
Robertson JD and Zhivotovsky B (2000) Nuclear events in Apoptosis. *J Struct Biol* **129:**346–358.
Sánchez-Alcázar JA, Ault JG, Khodjakov A and Schneider E (2000) Increased mitochondrial cytochrome c levels and mitochondrial hyperpolarization precede camptothecin-induced apoptosis in Jurkat cells. *Cell Death Differ* **7:**1090–1100.
Sawada S, Matsuoka S, Nokata K, Nagata H, Furuta T, Yokokura T and Miyasaka T (1991) Synthesis and antitumor activity of 20(S)-camptothecin derivatives: A-ring modified and 7,10-disubstituted camptothecins. *Chem Pharm Bull* **39:**3183–3188.
Shimizu T and Pommier Y (1997) Camptothecin-induced apoptosis in p53-null human leukemia HL60 cells and their isolated nuclei: effects of the protease inhibitors Z-VAD-fmk and dichloroisocoumarin suggest an involvement of both caspases and serine proteases. *Leukemia* **11:**1238–1244.
Solary E, Droin N, Bettaieb A, Corcos L, Dimanche-Boitrel MT and Garrido C (2000) Positive and negative regulation of apoptotic pathways by cytotoxic agents in hematological malignancies. *Leukemia* **14:**1833–1849.
Stennicke HR, Jürgensmeier JM, Shin H, Deveraux Q, Wolf BB, Yang X, Zhou Q, Ellerby HM, Ellerby LM, Bredesen D, et al. (1998) Pro-caspase-3 is a major physiologic target of caspase-8. *J Biol Chem* **273:**27084–27090.
Tang L, Boise LH, Dent P and Grant S (2000) Potentiation of 1-β-arabinofuranosylcytosine-mediated mitochondrial damage and apoptosis in human leukemia cells (U937) overexpressing Bcl-2 by the kinase inhibitor 7-hydroxystaurosporine (UCN-01). *Biochem Pharmacol* **60:**1445–1456.
Taylor ST, Hickman JA and Dive C (2000) Epigenetic determinants of drug resistance in tumors: regulation of Bcl-xL and Bax by tumor microenvironmental factors. *J Natl Cancer Inst* **92:**18–23.
Uhlmann EJ, D'Sa-Eipper C, Subramanian T, Wagner AJ, Hay N and Chinnadurai G (1996) Deletion of a nonconserved region of Bcl-2 confers a novel gain of function: suppression of apoptosis with concomitant cell proliferation. *Cancer Res* **56:**2506–2509.
Urasaki Y, Takebayashi Y and Pommier Y (2000) Activity of a novel camptothecin analogue, homocamptothecin, in camptothecin-resistant cell lines with topoisomerase I alterations. *Cancer Res* **60:**6577–6580.
Utz PJ and Anderson P (2000) Life and death decisions: regulations of apoptosis by proteolysis of signaling molecules. *Cell Death Differ* **7:**589–602.
Wolf D and Rotter V (1985) Major deletion in the gene encoding the p53 tumor antigen cause lack of p53 expression in HL-60 cells. *Proc Natl Acad Sci USA* **82:**790–794.
Zamzami N, Metivier D and Kroemer G (2000) Quantitation of mitochondrial transmembrane potential in cells and in isolated mitochondria. *Methods Enzymol* **322:**208–213.

Address correspondence to: Christian Bailly, INSERM U-524, Laboratorie de Pharmacologie Antitumorale du Centre Oscar Lambret, IRCL, Place de Verdun, 59045 Lille Cedex, France. E-mail: bailly@lille.inserm.fr